International Journal of Robotics and Automation (IJRA)
Vol. 4, No. 2, June 2015, pp. 98 – 108
ISSN: 2089-4856

A Safe Interaction of Robot Assisted Rehabilitation, Based on Model-Free Impedance Control with Singularity Avoidance

Iman Sharifi*, Heidar Ali Talebi*, and Ali Doustmohammadi*
*Electrical Engineering Department, Amirkabir University of Technology

Article Info

Article history:

Received Feb 9, 2015
Revised May 8, 2015
Accepted May 19, 2015

Keyword:

Tele-rehabilitation
Teleoperation
Haptic feedback
Nonlinear Control
Robotic Control

Corresponding Author:
Iman Sharifi
Amirkabir University of Technology
424 Hafez Ave, Tehran, Iran, 15875-4413
+98 21 64543398
imansharifi@aut.ac.ir

ABSTRACT

In this paper, a singularity-free control methodology for the safe robot-human interaction is proposed using a hybrid control technique in robotic rehabilitation applications. With the use of max-plus algebra, a hybrid controller is designed to guarantee feasible robot motion in the vicinity of the kinematic singularities or going through and staying at the singular configuration. The approach taken in this paper is based on model-free impedance control and hence does not require any information about the model except the upper bounds on the system matrix. The stability of the approach is investigated using multiple Lyapunov function theory. The proposed control algorithm is applied to PUMA 560 robot arm, a six-axis industrial robot. The results demonstrate the validity of the proposed control scheme.

1. INTRODUCTION

Robot assisted rehabilitation is becoming very popular among people who have suffered from a stroke due to proprioceptive neuromuscular facilitation procedure. In many cases, stroke causes an injury to the nervous system that causes disability in a person. In cases like this, the robot is not only a good substitute of a therapist for performing suitable exercises on the injured person but also it can perform repetitive and case-oriented exercises that are hard for the therapist to carryout. Repetitive and task-oriented exercises can improve muscular strength and movement coordination in patients with impairments due to neurological or orthopedic problems. A typical repetitive movement is the human gait. Treadmill training has been shown to improve gait and lower limb motor function in patients with locomotor disorders [1]. Manually assisted treadmill training was first used as a regular therapy for patients with spinal cord injury (SCI) or stroke around 15 years ago. Many clinical studies prove the effectiveness of the training, particularly in SCI and stroke patients [2].

Manual exercises have numerous limitations. The training is labor-intensive and therefore, training duration is usually limited by fatigue and therapist shortage [3]. Subsequently, the training sessions are shorter than what is required to achieve an optimal therapeutic outcome. Finally, manually-assisted exercises lack repeatability and measurement indexe of patient performance and progress.

In contrast to manually-assisted exercises, using robot assisted exercises, the duration and number of training sessions can be increased and the number of therapists required per patient can be reduced. Furthermore, the robot provides quantitative measure indexes and hence it allows the observation and judgment of the rehabilitation process.

Various robot assisted rehabilitation systems have been developed to support therapy of the upper extremities. Arm trainer from Hesse et al. [4], the arm robot from Cozens [5], the haptic display of the European project GENTLE/s [6] which is based on the FCS Haptic Master [7], the MIT-Manus [8] and [9], and the MIME (Mirror Image Movement Enhancer) arm therapy robot [10] are examples of such systems. ARMin is another rehabilitation robot system that is currently being developed for upper extremity treatments [2]. Since the patients limb is in direct contact with the robots

end-effector while training, the excessive interaction force may beat the ill limb. As a result, the robots end effector and interaction between the patients limb must be deliberately reckoned [11]. Recently, various force and position control schemes have been designed for robotic interaction tasks. Gorce and Guihard [12] have proposed a multi-link, position based impedance controller for implementation on a legged robot. Heinrichs et al. [13] have proposed a position based impedance controller for an existing hydraulic industrial robot, confirming their work experimentally. They used an actuator model to predict the torque produced from the pneumatic cylinders and the performance of the controller was demonstrated through simulation. Seul June [14] has used a double-loop system to improve the adaptability with the position feedback in the inner loop and to improve controller capability by tracking the desired impedance using the outer loop.

Impedance controllers are very applicable in the field of robotics and human-system interaction. They were first introduced by N. Hogan in 1985 [15]. The basic idea of the impedance control strategy applied to robot-aided treadmill training is to allow a variable deviation from a given leg trajectory rather than imposing a rigid gait pattern. The deviation depends on the patients effort and behavior.

In this paper a new approach for safe interaction of robot-assisted rehabilitation based on model-free impedance control is proposed. The impedance controller allows the robot to achieve a certain security and compliance. Also, a singularity-free approach methodology is combined with such a controller to solve the problem of boundary and interior singularity for safer interaction. The rest of the paper is organized as follows. In the next section, Max-Plus algebra which is used to implement the hybrid controller is briefly discussed. The controller design is discussed in Section III and the stability of the controller is investigated in Section IV. Finally, concluding remarks and future works are presented in Section V.

2. MAX-PLUS ALGEBRA

Max-Plus algebra is widely used to model behavior of systems that are discrete by nature, namely Discrete Event Systems (DEDS). The use of Max-Plus algebra structure gives these problems the characteristic of a linear algebra framework in which one can talk about notions like independence, eigenvalues, eigenvectors, and so on [16]. $\Re_{max}$ is defined as $\Re_{max} = \Re \cup \{-\infty\}$; $\oplus$ denotes the Max operation and $\otimes$ denotes the Plus operation.

Here the operations $\oplus$ and $\otimes$ are defined as [17]:

$$a \oplus b = max(a, b)$$

and

$$a \otimes b = a + b.$$

Moreover, the expression a^b in Max-Plus algebra corresponds to $a.b$ (Inner Product) in classical algebra. In this article, Max-Plus algebra is used to switch between two robot controllers in the system and is discussed in more detail in section IV.

3. CONTROLLER DESIGN

In this section the overall architecture of the controller is discussed. The controller consists of two major parts. The first part is inner loop controller. This part handles the common problem of the singularity in the robotic system and guarantees the singularity free motion control. The second part is the impedance control which deals with the exact tracking of both force and position tracking together.

3.1. Inner Loop Controller

Dynamical model of a robot arm with n joints is given by

$$M(q)\ddot{q} + C(q, \dot{q})\dot{q} + g(q) = u - \tau_d \tag{1}$$

where $M(q)$ is the $n \times n$ positive definite manipulator inertia matrix, u is the $n \times 1$ vector of applied torques, $C(q, \dot{q})\dot{q}$ is the $n \times 1$ centripetal and Coriolis terms, $g(q)$ is the $n \times 1$ vector of gravity term and, finally, $q = \{q_1, q_2, ..., q_n\}^T$ is the $n \times 1$ vector of joint displacements. Both joint space or task space can be used for controlling the robots. In joint space, a robot task is specified in an n-dimensional joint space denoted by q. Joint level controller can be formulated as

$$u_j = M(q)(\ddot{q}_d + K_{Vq}e_{q2} + K_{P_q}e_{q_1}) + (q, \dot{q})\dot{q} + g \tag{2}$$

where $e_q = [e_{q1}, e_{q2}]^T = [\ddot{q_d}, \dot{q_d}]^T$, K_{Vq} and K_{Pq} are feedback gain matrices . Therefore, equation of error in joint space is as follows

$$\begin{aligned} \dot{e}_{q_1} &= e_{q_2} \\ \dot{e}_{q_2} &= -K_{Pq} e_{q_1} - K_{Vq} e q_2 \end{aligned} \tag{3}$$

It is easy to prove that system given by (3) is locally asymptotically stable for suitable gain matrices K_{Pq}, K_{Vq}. So, system (3) can track any trajectories given as q^d, $\dot{q}^d$, $\ddot{q}^d$, regardless of the current robot configuration. Therefore, the joint level controller (2) is valid on the entire workspace.

Although the above fact is true on the entire workspace, it is desired to design the robot controllers in the task space because a robot task is generally represented by the desired end-effector position and its orientation. So, to design a task level controller, the robot model needs to be represented in terms of task level variables. Hence, the joint and task space acceleration can be utilized and related as $\ddot{x} = \dot{J}\dot{q} + J\ddot{q}$. Thus, the dynamics of the robot in terms of extended task space variables can be formulated as $MJ^{-1}(\ddot{x} - \dot{J}\dot{q}) + C(q, \dot{q})\dot{q} + g(q) = u$, where the Jacobian matrix is in square form ($n \times n$). The robot controller in task space can be described regarding to the desired path in task space, x^d, as follows

$$u_d = MJ^{-1}(\ddot{x}_d - \dot{J}\dot{q} + K_{Vx} e_{x2} + K_{Px} e_{x1}) + C\dot{q} + g \tag{4}$$

where $e_x = [e_{x1}, e_{x2}]^T = [x^d - x, \dot{x}_d - \dot{x}]$. The error dynamics in task space can be described as

$$\begin{aligned} \dot{e}_{x_1} &= e_{x_2} \\ \dot{e}_{x_2} &= -K_{Px} e_{x_1} - K_{Vx} e_{x_2} \end{aligned} \tag{5}$$

It is also straightforward to prove that system (5) is locally asymptotically stable for suitable gain matrices K_{Px}, K_{Vx}.

3.2. Outer Loop Controller (Impedance Controller)

For a safe human-robot interaction, the following passive impedance model is imposed to the robot arm [18]:

$$M_d(\ddot{q} - \ddot{q}_d) + C_d(\dot{q} - \dot{q}_d) + G_d(q - q_d) = -\tau_d \tag{6}$$

where M_d, C_d, G_d are the desired inertia, damping, and stiffness matrices respectively and q_d is the rest position of the robot manipulator.

The aim of the outer loop controller is to make the robot arm (1) dynamics track the impedance model given by (6). The detail of the controller design is given in [19] and only a brief description of the design is presented here.

The following error signal is first defined between the virtual system and the real system with the specified impedance (6), as in [20]:

$$w = M_d\ddot{e} + C_d\dot{e} + G_d e + \tau_d \tag{7}$$

where $e = q - q_d$. The aim of the controller is to make the error signal go to zero as time goes to infinity, that is

$$\lim_{t\to\infty} w(t) \to 0 \tag{8}$$

Hence, an augmented impedance error is defined as follows:

$$\bar{w} = K_f w = \ddot{e} + K_d\dot{e} + K_p e + K_f\tau_d \tag{9}$$

where $K_d = M_d^{-1}C_d$, $K_p = M_d^{-1}G_d$, $K_f = M_d^{-1}$.

Two positive definite matrices are defined as Υ and E such that

$$\begin{aligned} \Upsilon + \mathrm{E} &= K_d \\ \dot{\Upsilon} + \mathrm{E}\Upsilon &= K_p. \end{aligned} \tag{10}$$

Furthermore, define

$$\dot{\tau}_l + \mathrm{E}\tau_l = K_f\tau_d \tag{11}$$

Thus, (9) can be rewritten as:

$$\bar{w} = \ddot{e} + (\Upsilon + \mathrm{E})\dot{e} + (\dot{\Upsilon} + \mathrm{E}\Upsilon)e + \dot{\tau}_l + \mathrm{E}\tau_l \tag{12}$$

By defining

$$z = \dot{e} + \Upsilon e + \tau_l \tag{13}$$

The following can be obtained:

$$\bar{w} = \dot{z} + \mathrm{E}z \tag{14}$$

From (9) and (14), $z = 0$ will lead to $w = 0$. Finally, based on this fact, the aim of the control becomes

$$\lim_{t\to\infty} z(t) \to 0 \tag{15}$$

Now, consider the outer loop control input as follows:

$$\tau = \tau_s + \tau_f + \hat{\tau}_d \tag{16}$$

where τ_f and τ_s, are the feedback control torque and switching control torque, respectively. The corresponding elaborated expressions are given below.

An augmented state variable is first defined as follows

$$\dot{q}_r = \dot{q}_d - \Upsilon e - \hat{\tau}_l \tag{17}$$

where $\hat{\tau}_l$ is the estimator of τ_l and satisfies

$$\dot{\hat{\tau}}_l + \mathrm{E}\hat{\tau}_l = K_f \hat{\tau}_d \tag{18}$$

Furthermore, $\bar{z}$ and $\tilde{\tau}_l$ are defined as follows

$$\begin{array}{l} \bar{z} = \dot{e} + \Upsilon e + \hat{\tau}_l = z + \hat{\tau}_l \\ \tilde{\tau}_l = \hat{\tau}_l - \tau_l \end{array} \tag{19}$$

Using (17) and (19) one can obtain

$$\bar{z} = \dot{q} - \dot{q}_r \tag{20}$$

The above relation will be used in control performance analysis section. The switching control torque in (16) is given by

$$\tau_s = -(K_1 \left\|\ddot{q}_r\right\| + K_2 \left\|\dot{q}\right\| \left\|\dot{q}_r\right\| + K_3)\mathrm{sgn}(\bar{z}) \tag{21}$$

where K_1, K_2, K_3 are diagonal and positive definite matrices of large enough elements such that

$$\begin{array}{r} k_{1,i} \geq k_M,\ k_{2,i} \geq k_C,\ k_{3,i} \geq (k_G + k_d) \\ for\ \ i = 1, 2, ..., n \end{array} \tag{22}$$

The feedback control torque (16) is given by

$$\tau_f = -K\bar{z} \tag{23}$$

where K is a diagonal positive definite matrix with elements k_i, $i = 1, 2, ..., n$.

Remark 1 *When $k_{1,i}$, $k_{2,i}$, $k_{3,i}$, k_i are selected identical for $i = 1, ..., n$, (21) and (23) become fairly simple controllers from implementation point of view, however it may be required to use different $k_{1,i}$, $k_{2,i}$, $k_{3,i}$, k_i for better control performance in some cases.*

4. ANALYSIS OF THE SINGULARITIES

It is noted that the existence of task level controller (4) depends on the existence of J_0^{-1}. Singular configurations are the configurations in which J_0 has rank deficiencies. At singular configurations, J_0^{-1} does not exist. For a 6-DOF manipulator, which consists of a 3-DOF spherical wrist and a 3-DOF forearm, J, is a 6×6 matrix and a configuration is singular if and only if $det(J_0) = 0$. Both the arm and the wrist singularities can cause singularities and they can be decoupled into arm singularities and wrist singularities, respectively. The Jacobian could be decoupled in three parts instead of studying the determinant of J_0 [21]:

$$J_0 = \begin{bmatrix} I & U \\ 0 & I \end{bmatrix} \begin{bmatrix} I & 0 \\ 0 & \Psi \end{bmatrix} \begin{bmatrix} J_{11} & 0 \\ J_{21} & J_{22} \end{bmatrix} \tag{24}$$

The determinants of Ψ and U cannot be zero. Hence, the singularity conditions are $det(J_{22}) = 0$ and $det(J_{11}) = 0$. $det(J_{11}) = 0$ stands for the forearm singularity. Two singularity conditions can be obtained from the forearm

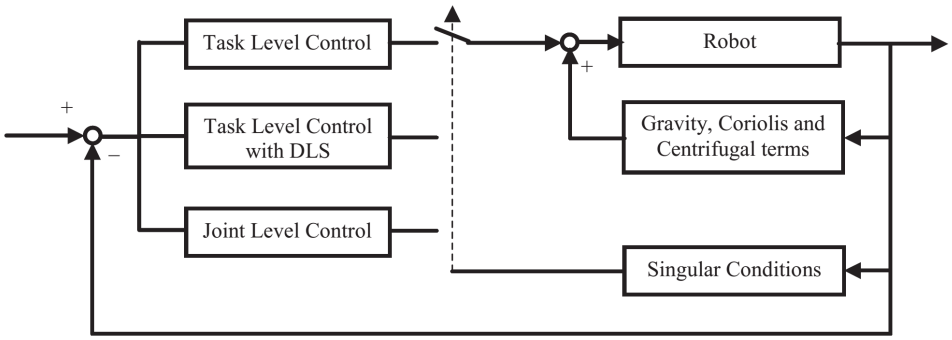

Figure 1. Framework for hybrid system controllers [22].

singularity. The so called "boundary singularity" appears when the elbow is fully extended or retracted and can be described by following equation

$$\gamma_b = d_4 c_3 - a_3 s_3 = 0 \tag{25}$$

The other singularity that is called "interior singularity", occurs when

$$\gamma_i = d_4 s_{23} + a_2 c_2 + a_3 c_{23} = 0 \tag{26}$$

The wrist singularity can be identified by checking the determinant of the matrix J_{22} to see if the following condition is satisfied

$$\gamma_w = -s_5 = 0 \tag{27}$$

When two joint axes are collinear, the wrist singularity occurs. Here s_i and c_i represent $\sin q_i$ and $\cos q_i$ respectively. The neighborhood of singularity is defined by positive constants $\varepsilon_b,\ \varepsilon_i,\ and\, \varepsilon_w$ that could be expressed as

$$|\gamma_b| \leq \varepsilon_b, \quad |\gamma_i| \leq \varepsilon_i, \quad |\gamma_w| \leq \varepsilon_w$$

5. ROBOTIC HYBRID CONTROLLER

In hybrid control systems, both continuous and discrete dynamic of the system are involved. The development of such systems is given by equations of motion that generally depends on both continuous and discrete variables. Fig. 1 shows a general framework for the hybrid system controllers. The hybrid controller is in form of hierarchical structure that includes a discrete and a continuous layer together. A discrete switching function is designed in order to select the appropriate continuous function for use. Singular configuration and the previous controller status determines the situation. When the robot gets close to the singular configuration, at the very first step the hybrid controller uses damped least squares to achieve an approximate motion of the end effector and then it will switch to joint level control. The general design procedure is discussed as follows.

The first step in the hybrid controller design is the partition of the workspace and the singularity analysis of the manipulator. For a given mechanical structures, the singular configuration and the corresponding singular condition vector Γ can be obtained.

The second step uses the definition of the subspaces to design the switching functions. Two switching function vectors are required. One is the switching function between region Ω_1 and region Ω_2 and the other one is the switching function between the regular region Ω_0 and region Ω_1. The switching functions can be written as:

$$m_{s1} = \operatorname{sgn}(\beta - |\gamma|) \oplus 0\,, \qquad \forall \gamma \in \Gamma \tag{28}$$

$$m_{s2} = m_{s2}(t^-)^{\operatorname{sgn}(\alpha+\delta-|\gamma|)\oplus 0} \oplus \operatorname{sgn}(\alpha - |\gamma|) \oplus 0, \quad \forall \gamma \in \Gamma \tag{29}$$

where $sgn(.)$ is a signum function. The switching function is a function of the singular conditions represented by Max-Plus Algebra. This part is designed to rule out the chattering feature of a switching controller.

The third step is the design of the continuous controllers. In this step three important fragments must be considered. In subspace Ω_0, matrix J is always invertible and the task level control (4) is effective in this subspace. In subspace Ω_2, the joint level controller is used. Finally, in region Ω_1, which is close to a singular configuration,

a feasible solution of inverse Jacobian can be obtained by pseudo-inverse or singular robust inverse (SRI). The task level controller (4) still can be used after replacing $J^{\dagger}$ with J^{-1}, where $J^{\dagger}$ is a kind of pseudo-inverse formulated by:

$$J^{\dagger} = (J^T.J + \lambda m_{s1} I)^{-1} J^T,$$

where λ is the damping factor and I is an identity matrix. Therefore, the controller in region Ω_1 can be represented by

$$u_d = MJ^{\dagger}(\ddot{x}^d - \dot{J}\dot{q} + K_{Vx}e_{x2} + K_{Px}e_{x1}) + c + g \tag{30}$$

The error dynamics of the system can be formulated by

$$\begin{aligned} \dot{e}_{x1} &= e_{x2} \\ \dot{e}_{x2} &= (I - K)(\ddot{x}^d - \dot{J}\dot{q}) - K(K_{Px}e_{x1} - K_{Vx}e_{x2}) \end{aligned} \tag{31}$$

Here the value of K is defined as $K = JJ^{\dagger}$. The stability analysis of controller (3.1) is discussed in [23]. Yet, it can be proved that the controller based on pseudo-inverse method will cause instability in subspace Ω_2 [24]. Although subspace Ω_2 could be very small, it cuts the dexterous workspace into pieces. If the robot cannot travel through subspace Ω_2, the singular configuration will greatly restrict the dexterous workspace. Consequently, joint level control will be utilized in subspace Ω_2 to stabilize the system.

With the continuous controllers in different subspaces and the switch functions, the next step is to formulate the hybrid robot motion controller in the entire workspace utilizing the switching conditions m_{s1} and m_{s2}:

$$u = (1 - m_{s2})u_d + m_{s2}u_j \tag{32}$$

where the switch function m_{sl} is within Eq. (28). The values of m_{s1} and m_{s2} determine the continuous controllers that should be used. m_{s2} takes the values of 1 or 0 and therefore u_d is the controller for subspace $\Omega_0 \cup \Omega_1$, and u_j is the controller for subspace $\Omega_0 \cup \Delta$. m_{s1} also takes the values of 1 or 0. When $m_{s1} = 0$, $u_d = u_t$ and therefore Eqs. (4) and (30) are the same. When m_{s1} equals unity, the damped least-square method is instantiated, and the inverse Jacobin is $J^{\dagger}$. Thus, the design of m_{s1} and m_{s2} is the discrete controller as discussed in the second step. The stability of the hybrid motion controller in the entire workspace should also be verified, based on the stability analysis of the continuous controllers in their respective region.

Finally, the last step of the hybrid controller design is the path planning of the continuous controllers. Given the desired path in the task space (x_d), controllers (30) and the task level controller (4) can be implemented. But, when the controller switches to u_d from u_j, the task representation q_d should be transformed to x_d by the forward kinematics equation $x_d = h(q_d)$. When the controller switches to u_j from u_d, the task representation x_d is transformed to q_d, which involves the inverse kinematics at singular configuration. At the vicinity of singular configuration, a suitable increment or decrement dx could result in a large increment or decrement dq. dq needs to be reparameterized in joint space to achieve the velocity and acceleration constraints. The continuity of joint velocities and task level velocities are also considered in the planning. After switching from task level control to joint level, the initial velocity for every joint is the joint velocity prior to switching.

6. ANALYSE OF STABILITY

This section discusses the stability of controller (32) when switching between the controllers in (30) and (2) is involved. To proceed further, the following assumption and properties are needed. Assumption 1: *The noise in torque measurement is bounded and known k_d , i.e., $\|\tilde{\tau}_d\| \leq k_d$, where $\tilde{\tau} = \hat{\tau}_d - \tau_d$ and $\hat{\tau}_d$ is the measurement of τ_d.*

Property 1 *The matrix $\dot{M}(q) - 2C(q, \dot{q})$ is a skew symmetric matrix if $C(q, \dot{q})$ is in the Christoffel form, i.e., $x^T(\dot{M}(q) - 2C(q, \dot{q}))x = 0$, $\forall x \in \Re^n$ [25].*

Property 2 *The matrix $M(q)$ is symmetric and positive definite.*

Property 3 *$\|M(q)\| \leqslant k_M$, $\|C(q, \dot{q})\dot{q}\| \leqslant k_C \|\dot{q}\|$ and $\|G(q)\| \leqslant k_G$, where k_M, k_C, k_G are positive scalars [18].*

Theorem 1 *Considering the robot dynamics described by (1), under Assumption 1, the control design (16) with (21) and (23) guarantees the following results:*

- *(i) $\lim_{t\to\infty} w = 0$ is bounded by $k_d\|M_d\|$, i.e., $\| \lim_{t\to\infty} w = 0 \leq k_d\|M_d\|$. When τ_d is zero, $k_d = 0$ indicates $\lim_{t\to\infty} \bar{w} = 0$.*

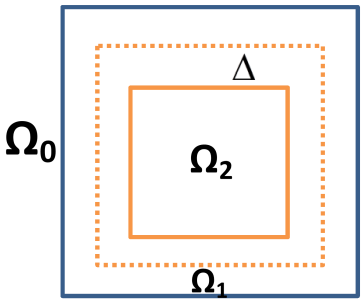

Figure 2. Workspace Partition.

- *(ii) all the signals in the closed-loop are bounded.*

Proof 1 *Consider the following Lyapunov function:*

$$W(t) = \frac{1}{2}\bar{z}^T M(q)\bar{z} \tag{33}$$

Taking the derivative of (33) gives

$$\begin{aligned}
&\dot{W}(t) = \bar{z}^T M(q)\dot{\bar{z}} + \tfrac{1}{2}\bar{z}^T \dot{M}(q)\bar{z} \\
&= \bar{z}^T M(q)\dot{\bar{z}} + \bar{z}^T C(q,\dot{q})\bar{z} \\
&= \bar{z}^T M(q)(\ddot{q} - \ddot{q}_r) + \bar{z}^T C(q,\dot{q})(\dot{q} - \dot{q}_r) \\
&= \bar{z}^T((M(q)\ddot{q} + C(q,\dot{q})\dot{q} + G(q)) \\
&-(M(q)\ddot{q}_r + C(q,\dot{q})\dot{q}_r + G(q))) \\
&= \bar{z}^T(-K\bar{z} - (K_1 \|\ddot{q}_r\| + K_2 \|\dot{q}_r\| \|\dot{q}\| + K_3)\mathrm{sgn}(\bar{z}) + \\
&+\widetilde{\tau}_d - (M(q)\ddot{q}_r + C(q,\dot{q})\dot{q}_r + G(q)))
\end{aligned} \tag{34}$$

where we have used Property 1 and Property 2 in the first equality and (20) in the second equality. Considering Property 3, we have

$$\begin{aligned}
&\bar{z}^T(M(q)\ddot{q}_r + C(q,\dot{q})\dot{q}_r + G(q) \\
&\leq \|\bar{z}\|(\|M(q)\ddot{q}_r\| + \|C(q,\dot{q})\dot{q}_r\| + \|G(q)\| \\
&\leq \|\bar{z}\|(\|M(q)\| \|\ddot{q}_r\| + \|C(q,\dot{q})\| \|\dot{q}_r\| + \|G(q)\| \\
&\leq \bar{z}^T(k_M \|\ddot{q}_r\| + k_C \|q_r\| \|\dot{q}_r\| + k_G)\mathrm{sgn}(\bar{z})
\end{aligned} \tag{35}$$

Similarly, from Assumption 1, we obtain

$$\bar{z}^T\tau_d \leq k_d\bar{z}^T\mathrm{sgn}(\bar{z}) \tag{36}$$

Substituting (35) and (36) into (34) results in

$$\begin{aligned}
&\dot{W}(t) \leq \bar{z}^T(-K\bar{z} - (K_1 \|\ddot{q}_r\| + K_2 \|\dot{q}_r\| \|\dot{q}\| \\
&+K_3)\mathrm{sgn}(\bar{z})) + kd\bar{z}^T\mathrm{sgn}(\bar{z}) \\
&+\bar{z}^T(k_M \|\ddot{q}_r\| + k_C \|\dot{q}_r\| \|\dot{q}\| + k_G)\mathrm{sgn}(\bar{z}) \\
&= -K\bar{z}^T\bar{z} - \bar{z}^T((K_1 - k_M I_n) \|\ddot{q}_r\| \\
&+(K_2 - k_C I_n) \|\dot{q}_r\| \|\dot{q}\| \\
&+(K_3 - k_G I_n - k_d I_n))\mathrm{sgn}(\bar{z}) \\
&= -K\bar{z}^T\bar{z} - (K_1 - k_M I_n) \|\ddot{q}_r\| \bar{z}^T\mathrm{sgn}(\bar{z}) \\
&-(K_2 - k_C I_n) \|\dot{q}_r\| \|\dot{q}\| \bar{z}^T\mathrm{sgn}(\bar{z}) \\
&-(K_3 - k_G I_n - k_d I_n)\mathrm{sgn}(\bar{z}) \leq 0
\end{aligned} \tag{37}$$

where I_n denotes a n-dimension identity matrix. (37) indicates that W is monotonically decreasing. Besides, suppose that $\bar{z}(0)$ is bounded, which comes from the assumption that $e(0) = 0$ and $\hat{\tau}(0) = 0$, then $W(0)$ is bounded since $\|M(q)\|$ is bounded. Therefore, W will converge to a non-negative fixed value, and thus we have

$$\lim_{t\to\infty} \dot{W} = 0 \tag{38}$$

Immediately, we have the following inequality

$$\dot{W} \leq -K\bar{z}^T\bar{z} \leq 0$$

Figure 3. D-H Parameter of PUMA 560.

i	θ_i	α_i	a_i	d_i
1	θ_1	*-90*	*0*	*0*
2	θ_2	*0*	a_2	d_2
3	θ_3	*90*	a_3	*0*
4	θ_4	*-90*	*0*	d_4
5	θ_5	*90*	*0*	*0*
6	θ_6	*0*	*0*	d_6

that leads to

$$\lim_{t\to\infty} \bar{z} = 0 \tag{39}$$

Furthermore, with the definition of $\bar{z}$ in (19), one can write

$$\lim_{t\to\infty} z = \lim_{t\to\infty} \tilde{\tau}_l \tag{40}$$

From (40), (9), (14) and Assumption 1, we finally obtain

$$\left\| \lim_{t\to\infty} w(t) \right\| \leq k_d \left\| M_d \right\|$$

which completes the proof.

Theorem 2 *Assume joint level controller (2) is asymptotically stable in workspace and task level controller (4) is uniformly ultimate bounded in region Ω_1. There exists a constant $\delta > 0$, as shown in Fig. 2 and a Δ, such that the hybrid robot motion controller (32) is ultimate-bounded in the entire workspace of the robot.*

7. SIMULATION

Currently most industrial and practical manipulators are six or fewer degrees-of-freedom (DOF). These manipulators are usually classified kinematically on the basis of the forearm or first three joints, while, the wrist being described separately. In this article it is assumed that the process of rehabilitation on the patient is accomplished using the popular PUMA 560. The general form of Jacobian matrix of this robot is as follows

$$\mathbf{J_E} = \begin{bmatrix} & 0 & d_6 \cdot z_{Ek} & -d_6 \cdot z_{Ej} \\ \mathbf{I}_3 & -d_6 \cdot z_{Ek} & 0 & d_6 \cdot z_{Ei} \\ & d_6 \cdot z_{Ej} & -d_6 \cdot z_{Ei} & 0 \\ \mathbf{0}_{3\times3} & & \mathbf{I}_3 & \end{bmatrix} \cdot \mathbf{J_W} \tag{41}$$

where J_E is

$${}^0\mathbf{J_W} = \begin{bmatrix} {}^0\mathbf{J}_{11} & \mathbf{0}_{3\times3} \\ {}^0\mathbf{J}_{21} & {}^0\mathbf{J}_{22} \end{bmatrix} \tag{42}$$

*A constant force is acting on the patient arm. The proposed controller, stabilizes the end effector force with a reasonable torques acting on joints. Simulation results are sown in Fig. (**??**). As can be seen from the figure ,.*

8. CONCLUDING REMARKS AND FUTURE WORKS

In this work, the human-robot interaction has been investigated and a mixed singularity-free and model-free impedance model has been simulated on the 6-DOF PUMA 560 robot to guarantee the interaction stability. The performance of the proposed method has been discussed through rigorous analysis. Simulation results on the robot arm validate the proposed method.

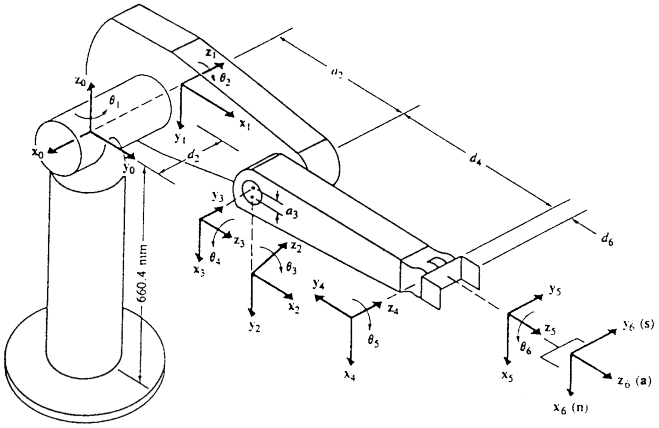

Figure 4. The 6-DOF PUMA manipulator [26].

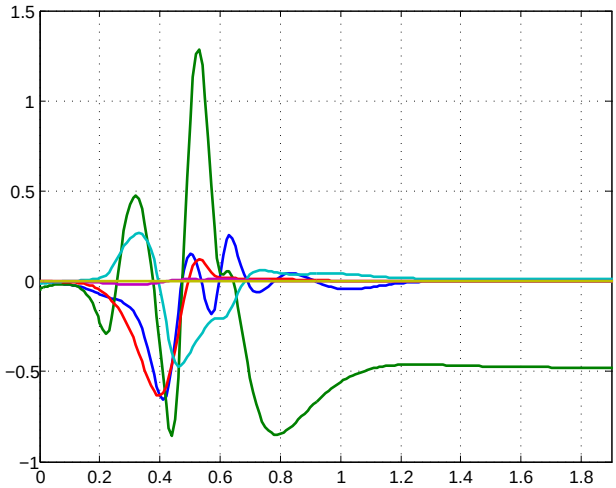

Figure 5. Torques of the joints

REFERENCES

[1] *R. Robert and et al, "Patient-cooperative strategies for robot-aided treadmill training: first experimental results,"* Neural Systems and Rehabilitation Engineering, IEEE Transactions on*, 2005.*

[2] *A. Gmerek, "Design of the robotic exoskeleton for upper-extremity rehabilitation,"* Pomiary, Automatyka, Robotyka*, vol. 17, pp. 97–101, 2013.*

[3] *J. R. Steadman, "Rehabilitation of first-and second-degree sprains of the medial collateral ligament,"* The American Journal of Sports Medicine*, 1979.*

[4] *S. Hesse, G. Schulte-Tigges, M. Konrad, A. Bardeleben, and C. Werner, "Robot-assisted arm trainer for the passive and active practice of bilateral forearm and wrist movements in hemiparetic subjects,"* Archives of physical medicine and rehabilitation*, vol. 84, no. 6, pp. 915–920, 2003.*

[5] *J. Cozens, "Robotic assistance of an active upper limb exercise in neurologically impaired patients,"* IEEE Trans. Rehab. Eng.*, 1999.*

[6] *W. Harwin, R. Loureiro, F. Amirabdollahian, M. Taylor, G. Johnson, E. Stokes, S. Coote, M. Topping, and C. Collin, "The gentle/s project: a new method for delivering neuro-rehabilitation. assistive technology added value to the quality of life,"* IOS Press*, 2001.*

[7] *J.-S. Oh, Y.-M. Han, S.-R. Lee, and S.-B. Choi, "A 4-dof haptic master using er fluid for minimally invasive surgery system application,"* Smart Materials and Structures*, vol. 22, no. 4, p. 045004, 2013.*

[8] *H. I. Krebs and et al., "Rehabilitation robotics: pilot trial of a spatial extension for mit-manus,"* Journal of NeuroEngineering and Rehabilitation*, 2004.*

[9] *T. Nef, R. Riener, R. Müri, and U. P. Mosimann, "Comfort of two shoulder actuation mechanisms for arm therapy exoskeletons: a comparative study in healthy subjects,"* Medical & biological engineering & computing*, pp. 1–9.*

[10] *R. Riener, T. Nef, and G. Colombo., "Robot-aided neurorehabilitation of the upper extremities,"* Medical and Biological Engineering and Computing*, 2005.*

[11] *Krebs, H. I., and et al., "Rehabilitation robotics: Performance-based progressive robot-assisted therapy,"* Autonomous Robots*, 2003.*

[12] *G. P and G. M., "Joint impedance pneumatic control for multilink systems,"* ASME Journal of Dynamic Systems, Measurement and Control*, 1999.*

[13] *B. Heinrichs, N. Sepehri, and A. Thornton-Trump, "Position-based impedance control of an industrial hydraulic manipulator,"* Control Systems, IEEE*, vol. 17, no. 1, pp. 46–52, 1997.*

[14] *S. Jung, "Experimental studies of neural network impedance force control for robot manipulators,"* IEEE Conf. On Robotics and Automations*, 2001.*

[15] *N. Hogan, "Impedance control: An approach to manipulation: Part illapplications,"* Journal of dynamic systems, measurement, and control*, 1985.*

[16] *A. Doustmohammadi, "Modeling and analysis of production systems," Ph.D. dissertation, Georgia Institute of Technology, 2009.*

[17] *P. Butkovič,* Max-linear systems: theory and algorithms*. Springer, 2010.*

[18] *A. Tayebi, "Adaptive iterative learning control for robot manipulators,"* Automatica*, vol. 40, no. 7, pp. 1195–1203, 2004.*

[19] *Y. Li, C. Yang, and S. S. Ge, "Learning compliance control of robot manipulators in contact with the unknown environment," in* Automation Science and Engineering (CASE), 2010 IEEE Conference on*. IEEE, 2010, pp. 644–649.*

[20] *D. Wang and C. C. Cheah, "An iterative learning-control scheme for impedance control of robotic manipulators,"* The International Journal of Robotics Research*, vol. 17, no. 10, pp. 1091–1104, 1998.*

[21] *F. Cheng, T. Hour, Y. Sun, and T. H. Chen, "Study and rosolution of singularities for a 6 dof puma manipulators."*

[22] *N. XI and J. TAN, "A hybrid robot motion task level control system," Nov. 1 2002, wO Patent 2,002,085,581.*

[23] *F. Caccavale, C. Natale, B. Siciliano, and L. Villani, "Resolved-acceleration control of robot manipulators: A critical review with experiments,"* Robotica*, vol. 16, no. 5, pp. 565–573, 1998.*

[24] *M. Kircanski, N. Kircanski, D. Lekovic, and M. Vukobratovic, "An experimental study of resolved acceleration control of robots at singularities: Damped least-squares approach,"* Journal of dynamic systems, measurement, and control*, vol. 119, no. 1, pp. 97–101, 1997.*

[25] *J. J. Craig, "Introduction to robotics: mechanics and control," 2004.*

[26] *K. S. Fu, R. C. Gonzalez, and C. Lee,* Robotics*. McGraw-Hill Book, 1987.*

BIOGRAPHIES OF AUTHORS

Iman Sharifi *received the B.Sc degree from Amirkabir University of Technology, Tehran, Iran, in 2009, and the M.Sc. degree from Amirkabir University of Technology, Tehran, Iran, in 2012, both in electrical engineering. He is currently working toward the Ph.D. degree in electrical engineering, at Amirkabir University of Technology, Montreal, Tehran, Iran. His research interests include telerehabilitation, teleoperation, robotics, control of nonlinear systems, robust control, and adaptive control. He is affiliated with IEEE as student member. In TELKOMNIKA, IAES journals, and other scientific publications, he has served as invited reviewer. Besides, he is also involved in NGOs, student associations, and managing non-profit foundation. Further info on his homepage: http://ele.aut.ac.ir/ imansharifi/*

Ali Talebi *received the B.S. degree in electronics from Ferdowsi University, Mashhad, Iran, in 1988, the M.Sc. degree in electronics (with first class honors) from Tarbiat Modarres University, Tehran, Iran, in 1991, and the Ph.D. degree in electrical and computer engineering from Concordia University, Montreal, QC, Canada, in 1997. He held several postdoctoral and research positions at Concordia University and University of Western Ontario, before joining Amirkabir University of Technology in 1999 where he is currently an Associate Professor. From 2002 to 2004, he also served as the Head of Control Systems Group in Amirkabir University. His research interests include control, robotics, fault diagnosis and recovery, intelligent systems, adaptive control, non-linear control, and real-time systems.*

Ali Doustmohammadi *received his B.S. and M.S. degrees in Electrical Engineering from Oregon State University in 1988 and 1991, respectively and the Ph.D. degree from School of Electrical And Computer Engineering, Georgia Institute of Technology in 1995. His main research interests are: modeling and analysis of production systems, discrete event dynamic systems, multivariable control, system identification, robotics, and industrial automation. Dr. Doustmohammadi, after spending 8 years in different industries in USA, joined Amirkabir University of Technology, Tehran, Iran in 2003.*